



Numerical study of a broadband metamaterial absorber using a single split circle ring and lumped resistors for X-band applications

Cite as: AIP Advances **10**, 035326 (2020); <https://doi.org/10.1063/1.5143915>

Submitted: 02 January 2020 . Accepted: 09 March 2020 . Published Online: 27 March 2020

Thi Quynh Hoa Nguyen , Thi Kim Thu Nguyen, Thanh Nghia Cao, Hugo Nguyen , and Long Giang Bach

COLLECTIONS

Paper published as part of the special topic on [Chemical Physics](#), [Energy, Fluids and Plasmas](#), [Materials Science](#) and [Mathematical Physics](#)



View Online



Export Citation



CrossMark

ARTICLES YOU MAY BE INTERESTED IN

[Numerical study of a wide incident angle- and polarisation-insensitive microwave metamaterial absorber based on a symmetric flower structure](#)

AIP Advances **9**, 065318 (2019); <https://doi.org/10.1063/1.5098005>

[Design, modeling, and fabrication of a new compact perfect metamaterial X-band absorber](#)

AIP Advances **10**, 025328 (2020); <https://doi.org/10.1063/1.5143934>

[Ultra-broadband microwave metamaterial absorber](#)

Applied Physics Letters **100**, 103506 (2012); <https://doi.org/10.1063/1.3692178>



NEW: TOPIC ALERTS

Explore the latest discoveries in your field of research

[SIGN UP TODAY!](#)

Numerical study of a broadband metamaterial absorber using a single split circle ring and lumped resistors for X-band applications

Cite as: AIP Advances 10, 035326 (2020); doi: 10.1063/1.5143915

Submitted: 2 January 2020 • Accepted: 9 March 2020 •

Published Online: 27 March 2020





View Online



Export Citation



CrossMark

Thi Quynh Hoa Nguyen,^{1,a)}  Thi Kim Thu Nguyen,¹ Thanh Nghia Cao,¹ Hugo Nguyen,² 
and Long Giang Bach^{3,a)}

AFFILIATIONS

¹School of Engineering and Technology, Vinh University, 182 Le Duan, Vinh City 460000, Vietnam

²Department of Materials Science and Engineering, Uppsala University, Uppsala 75121, Sweden

³NTT Hi-Tech Institute, Nguyen Tat Thanh University, Ho Chi Minh City 700000, Vietnam

^{a)}Authors to whom correspondence should be addressed: ntqhoa@vinhuni.edu.vn and blgiang@ntt.edu.vn

ABSTRACT

We report a numerical study on the design of a broadband metamaterial absorber (MMA) with a single layer of metal–dielectric–metal based on an FR-4 substrate for X-band applications. The MMA structure consists of a periodic array of a split circle ring and lumped resistors coupled within split segments. The MMA structure achieves a broadband absorption response in the frequency range of 7.8–12.6 GHz with an absorptivity of above 90% under normal incidence for all polarization angles. The absorptivity remains above 70% in the frequency range of 6.8–11.8 GHz at wide incident angles from 0° to 30° for both transverse electric and transverse magnetic polarizations. The physical mechanism of the absorber is explained by the electric and the surface current distributions that, in turn, are significantly affected by magnetic resonance.

© 2020 Author(s). All article content, except where otherwise noted, is licensed under a Creative Commons Attribution (CC BY) license (<http://creativecommons.org/licenses/by/4.0/>). <https://doi.org/10.1063/1.5143915>

INTRODUCTION

Metamaterial absorbers (MMAs) have been extensively studied for various applications such as sensors, solar cells, and electromagnetic interference (EMI) and radar cross section (RCS) reduction^{1–6} ever since a thin perfect microwave MMA was reported by Landy *et al.* in 2008.⁷ However, in reality, the design of MMAs for a suitable operating frequency band, a reasonable bandwidth, wide-angle tolerance, polarization insensitivity, a low profile, and an easy fabrication process is challenging. A perfect MMA normally exhibits a narrow bandwidth due to its resonant features. Therefore, many efforts have been taken on bandwidth enhancement of MMAs in order to make them more usable in practical applications.

Recently, different methods have been developed to extend the absorption band based on combination of various absorption peaks such as arranging different sizes/shapes of resonant elements or

stacking them in sequence metallic–dielectric pairs.^{8–13} Theoretically, many of these methods have been proved feasible by means of simulation, but difficulty and high cost of fabrication are usually the practical problems for them to be realized. More recently, a high impedance surface absorber based on loading lumped resistors was demonstrated as an easy method for the extending absorption band.^{14–20} Shang *et al.*, for example, presented a lumped resistor loaded double-square-loop microwave absorber composed of two dielectric layers, which could realize a fractional bandwidth of 126.8% with a reflection coefficient less than –10 dB.¹⁴ A similar design using double dielectric layers with four lumped resistors as the frequency selective surface was proposed to realize the broadband absorber in the operating frequency ranging from 7.6 GHz to 18.3 GHz.¹⁵ Cong *et al.* demonstrated a double layered absorber formed by loading four lumped resistors into symmetric split rings on the top metallic layer, which showed an ultra-wideband absorbance in the frequency range from 4 GHz to 22 GHz.¹⁶

Furthermore, Bağmancı *et al.* proposed a multilayered absorber structure composed of three metallic layers separated by two dielectric layers and four lumped resistors loaded on the top metallic layer and four short-pins connecting the top and the middle metallic layers, which exhibited a perfect absorption between 4 GHz and 16 GHz.¹⁸ However, the main drawback of these sophisticated structures is high thicknesses because of their many layers and thus difficulty in manufacturing. Recently, Chen *et al.* proposed an eight lumped resistor loaded double-ring microwave absorber composed of a single dielectric layer, which could achieve 7.60 GHz wide absorption from 8.87 GHz to 16.47 GHz with absorptivity higher than 90%.¹⁷ Furthermore, Nguyen *et al.* proposed a broadband microwave absorber made of an eight-resistive-aim cell, which achieved an absorption higher than 95% in the frequency range of 8.2–13.4 GHz for X-band applications.²⁰ However, these structures still required a large number of lumped resistors that posed a certain complexity in large-scale fabrication.

In this paper, we proposed a simple design of single layer broadband MMAs based on a split circle ring (SCR) loaded with four lumped resistors for X-band applications. The absorption mechanism and absorption properties of the proposed MMA are numerically studied.

STRUCTURE DESIGN AND METHODS

The unit cell of the proposed MMA is shown in Fig. 1(a). Its structure consists of a periodic array of an SCR. The top and the bottom layers are made of copper with an electric conductivity of $5.96 \times 10^7 \text{ S m}^{-1}$ and a thickness (t) of 0.035 mm. The SCR on the top layer is loaded with four lumped resistors in the gaps between the four sectors. The bottom copper layer, acting as the ground to block

the transmission, covers the entire backside of the FR-4 dielectric substrate, which has a relative dielectric constant of 4.3 and a loss tangent of 0.025.

In order to study the physics behind the absorption mechanism, an equivalent circuit model of a unit cell of the MMA was established using transmission line theory,^{21–25} as depicted in Fig. 1(b). Part A represents the transmission line of free space with a characteristic impedance of Z_0 , while part C represents a shorted transmission line for the FR-4 substrate. Part B consists of an RLC circuit, which represents the component of the metal top layer and lumped resistors. The absorbance of the proposed MMA is given by

$$A(\omega) = 1 - R(\omega) = 1 - \left| \frac{Z_{in}(\omega) - Z_0}{Z_{in}(\omega) + Z_0} \right|^2, \tag{1}$$

where

$$\frac{1}{Z_{in}(\omega)} = \frac{1}{Z_m(\omega)} + \frac{1}{Z_d(\omega)}, \tag{2}$$

$$Z_m(\omega) = R + j\omega L + \frac{1}{j\omega C}, \tag{3}$$

$$Z_d(\omega) = j\sqrt{\frac{\omega_r \omega_0}{\epsilon_r \epsilon_0}} \tan(k_r h), \tag{4}$$

$$k_r = k_0 / \sqrt{\epsilon_r \omega_r}, \tag{5}$$

and ϵ_0 and ϵ_r are the relative permittivities, ω_0 and ω_r are the relative permeabilities, and k_0 and k_r are the wavenumbers of the free space and the dielectric substrate, respectively.

From Eq. (1), $A(\omega)$ can be written as

$$A(\omega) = \frac{4Z_0[\text{Re}(Z_{in}(\omega)) + i\text{Im}(Z_{in}(\omega))]}{[\text{Re}(Z_{in}(\omega)) + i\text{Im}(Z_{in}(\omega))]^2 + 2Z_0[\text{Re}(Z_{in}(\omega)) + i\text{Im}(Z_{in}(\omega))] + Z_0^2}. \tag{6}$$

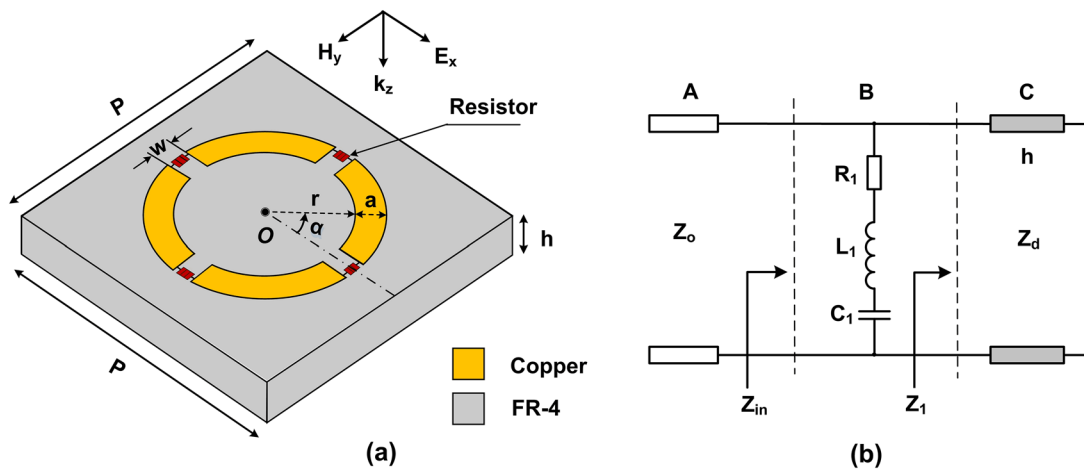


FIG. 1. Schematic of a unit cell of the proposed MMA: (a) 3D-view and (b) its equivalent circuit model.

Equation (6) can be simply rewritten as proposed by Li *et al.* as follows:¹⁹

$$A(\omega) = \frac{2Z_0}{\text{Re}(Z_{in}(\omega)) + i\text{Im}(Z_{in}(\omega)) + Z_0}, \quad (7)$$

where $\text{Re}(Z_{in}(\omega))$ and $\text{Im}(Z_{in}(\omega))$ are the real part and the imaginary part of $Z_{in}(\omega)$, respectively. According to Eq. (1), in order to obtain the perfect absorption [$A(\omega) = 1$] over all frequencies, the impedance matching condition $Z_{in}(\omega) = Z_0$ should be satisfied. This condition can be achieved when $\text{Re}(Z_{in}(\omega)) = Z_0 = 377 \Omega$ and $\text{Im}(Z_{in}(\omega)) = 0$, according to Eq. (7).

Based on the analysis of transmission line theory, the value of $Z_{in}(\omega)$ depends on size and shape of the resonant structure, the FR-4 substrate thickness, and the lumped resistances of MMA unit cells. Therefore, by tailoring the sizes of the resonant structure, the FR-4 substrate thickness, and the lumped resistances of MMA unit cells, the impedance matching condition can be obtained, and the perfect absorption can be achieved. To optimize the design, full-wave electrodynamic modeling was performed using the commercial Computer Simulation Technology (CST) Microwave Studio 2013²⁶ based on the finite integration technique (FIT). In this study, the boundary conditions are fixed to a unit cell for x and y directions and open for the z direction. A waveguide port is created in front of the configuration, and the electromagnetic wave is propagated at normal incidence to the surface. Good agreement between CST simulations and experimental results of MMAs was recently reported;^{27–32} therefore, the CST simulation method is also used in this work. It starts with determining the value of the lumped resistors and then dimensions of the MMA unit cells. By this order, the MMA can be systematically tuned for a wide absorption band with a higher absorbance in the entire X-band.

RESULTS AND DISCUSSION

Figure 2 shows different steps of the MMA's design. At first, absorption spectra of the MMA were investigated for different lumped resistor values (R) in the range of 190–310 Ω , as shown in Fig. 2(a). The initial dimensional parameters of the unit cells are $P = 16.6$, $r = 4.5$ mm, $a = 1.5$ mm, $h = 3.2$ mm, and $w = 1$ mm. It can be seen that the widest absorption band with absorptivity >90% can be obtained when $R = 250 \Omega$. From this value, the thickness (h) of the FR-4 substrate is next to be optimized. Figure 2(b) shows the absorption spectra vs h , which varies between 2.8 mm and 3.6 mm with an equal step of 0.2 mm. It can be seen that when the thickness of the dielectric substrate is increased, the absorption frequency range shifts to a higher frequency band, and this is in agreement with the results reported in Ref. 33. From this result, the thickness $h = 3.2$ mm is selected for absorptivity >90% on the entire X-band. The effect of the inner radius (r) and width (a) of the SCR on the absorption can be investigated now as the other structural parameters are kept fixed, as shown in Figs. 2(c) and 2(d). The absorption band shifts to the lower frequency bandwidth, increasing r from 3.9 mm to 5.1 mm, as seen in Fig. 2(c). Furthermore, the absorptivity of the highermost absorption frequency decreases dramatically with increasing r from 4.5 mm to 5.1 mm; thus, the widest absorption bandwidth can be achieved with $r = 4.5$ mm. Similarly, the absorption frequency band shows a red-shift with increasing a values from

0.9 mm to 1.8 mm, as shown in Fig. 2(d). The red-shift of the resonant frequency band is mainly due to the increase in the effective inductance due to the increase in the size of a .^{34,35} According to the equivalent RLC circuit, the resonant frequency is determined by $f_0 = 1/\sqrt{2\pi\sqrt{LC}}$.³⁵ Therefore, the increase in the inductance corresponding to the increase in the size of r and a causes the red-shift of the resonant frequency band. However, the widest bandwidth with absorptivity >90% is obtained with $a = 1.5$ mm. To summarize, the optimized values for the designed MMA for the X-band are found to be $R = 250 \Omega$, $h = 3.2$ mm, $r = 4.5$ mm, $a = 1.5$ mm with $P = 16.6$ mm, and $w = 1$ mm. It should be noted that it is feasible to use the conventional materials of the FR-4 substrate with a thickness of 3.2 mm for manufacturing of the designed MMA. Due to the fact that the size of the resonant structure of this MMA is in the millimeter range, the manufacturing process can be implemented based on the well-known photolithography technique.^{18,20,21,35–41} The chip resistors can be soldered using surface-mounting technology.^{20,21,41} The experimental setup for absorption measurement can be implemented as previously reported.^{18,20,41} It has been shown that results from CST simulations and from experiments of MMAs with lumped resistors are in good agreement.^{35–38}

To gain insights into the role of lumped resistors in the designed MMA structure, the absorption characteristics of the MMA structures with and without lumped resistors are investigated. Figure 3 shows the results of this investigation at normal incidence under transverse electric (TE) polarization. It can be seen that the MMA without lumped resistors provides two absorption peaks at 8.5 GHz and 12.5 GHz with an absorption intensity of 26.1% and 93.9%, respectively. The MMA structure with four lumped resistors exhibits a broadband absorption performance with absorptivity >90% in the broader frequency range from 7.8 GHz to 12.6 GHz, entirely covering the X-band of 8.0–12.0 GHz. Two distinct absorption peaks are found at 9.1 GHz and 12.2 GHz, corresponding to the absorption intensity of ~97.9%, and ~99.8%, respectively. It is evidently clear that the four lumped resistors play an important role in improving the bandwidth and the absorption intensity of the MMA. The mechanism of this phenomenon can be explained using the equivalent RLC circuit, meaning that the operating bandwidth of the MMA structure can be calculated using the following equation:

$$BW = \frac{f_0}{Q_C} = \frac{R}{2\pi L}, \quad (8)$$

where Q_C is the losses in the metallic patch, and f_0 , L , C , and R is the angular resonant frequency, inductance, capacitance, and resistance of the circuit, respectively ($f_0 = 2\pi\sqrt{LC}$).^{35,42}

From Eq. (8), it is clear that for the MMA structure with lumped resistors, the value of R is proportional to the bandwidth. It was also recently reported that the absorption peaks are combined in order to form the broadband absorption response in MMAs using lumped resistors.³⁵ Moreover, the combination of absorption peaks can improve the absorption intensity.

In order to analyze the absorption performance of the MMA, the relative absorption bandwidth (RAB) is calculated using the following equation, where f_U and f_L are the upper and the lower frequencies corresponding to the absorption band with an absorption intensity above 90%. The MMA achieves a high absorption performance with a RAB of up to 47%, which is higher than that of the

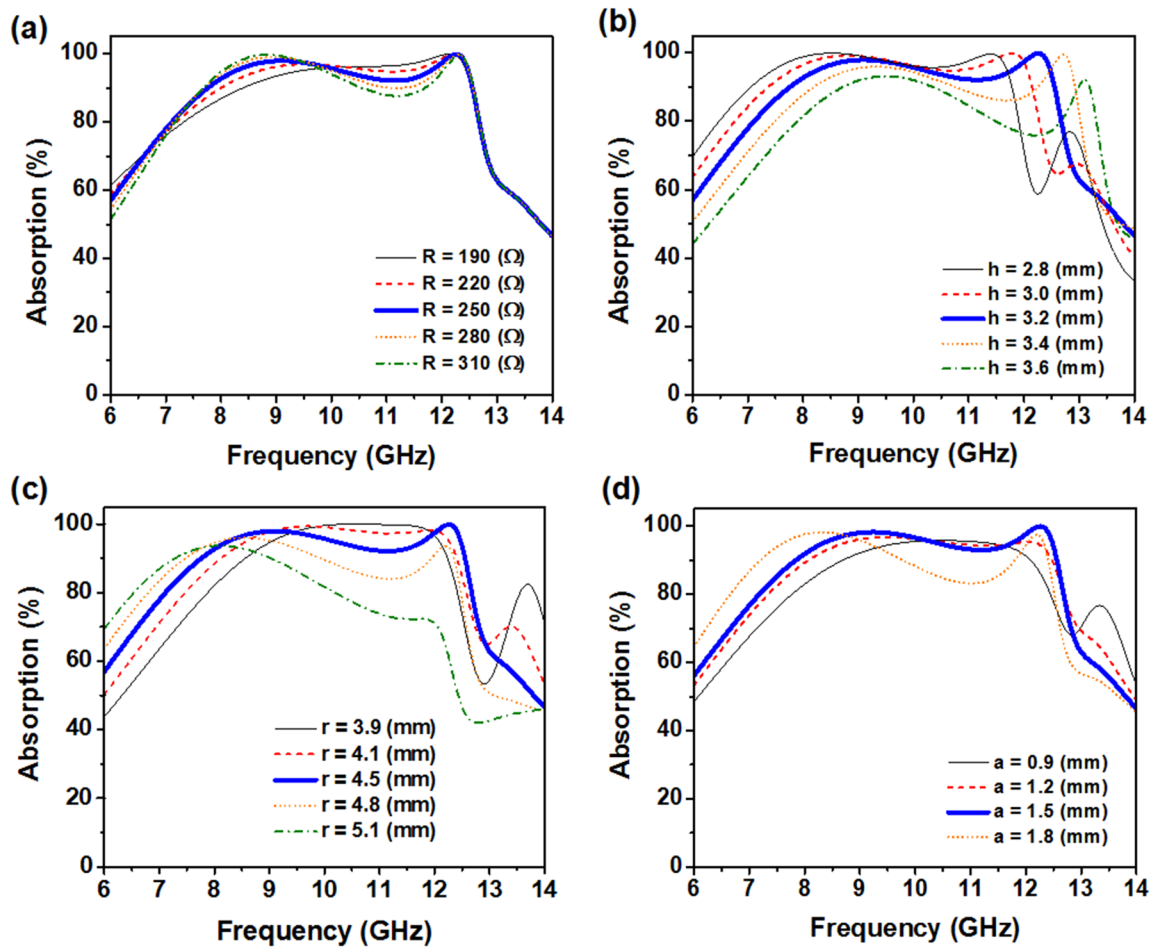


FIG. 2. Absorption spectra of the proposed MMA for various (a) lumped resistor values (R) and structural parameters: (b) h , (c) r , and (d) a for TE polarization under normal incidence.

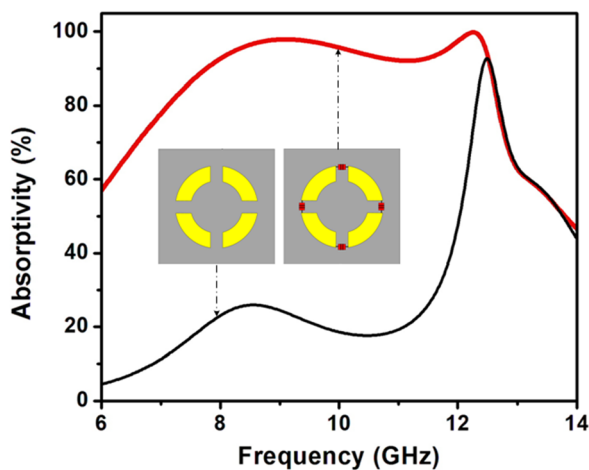


FIG. 3. Absorption spectra of the designed MMA structures with and without lumped resistors under normal incidence for TE polarization.

previously reported works,^{43,44}

$$RAB = 2 \times \frac{f_U - f_L}{f_U + f_L} \tag{9}$$

At the operating frequency band, the impedance matching between the free space and the MMA should occur in order to obtain a near perfect absorption. To determine impedance matching, the normalized input impedance (Z) of the MMA is investigated. Figure 4 shows the simulated normalized input impedance (Z), derived from Eq. (7), and the normalized input impedance of the MMA calculated based on the effective medium interference theory is given by the following equation:^{15,19,35,38,45-47}

$$Z = \sqrt{\frac{(1 + S_{11})^2 - S_{21}^2}{(1 - S_{11})^2 - S_{21}^2}} = \frac{1 + S_{11}}{1 - S_{11}} \tag{10}$$

As can be seen in Fig. 4, the calculated normalized input impedance coincides with the simulated one. Moreover, the imaginary and the real part of the normalized input impedance are

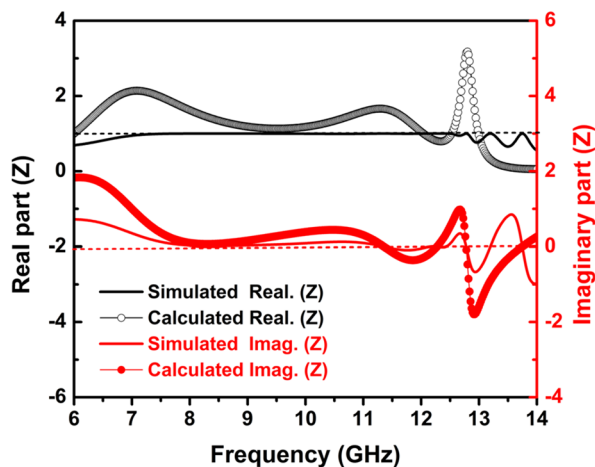


FIG. 4. The simulated and calculated normalized input impedance (Z) of the proposed MMA under normal incidence.

nearly 0 and 1, respectively, in the resonant frequency range, which confirms that the impedance matching between the free space and the MMA is successful. It indicates that the absorption mechanism of the designed MMA with loaded lumped resistors can be explained by the effective medium interference theory.

To study the absorption performance of the MMA, the effect of the incidence and the polarization angles on the absorption spectra under both transverse electric (TE) and transverse magnetic (TM) polarizations is investigated. Figure 5 shows that the absorption spectra of the MMA are dependent on the incident angle and that the high absorption intensity maintains over a wide range of incident angles for both TE and TM polarizations. For TE polarization, the absorptivity of the MMA decreases slightly with increasing incident angle from 0° to 45° . At an incident angle of 45° , the absorptivity is still higher than 80% in the frequency range of 8.0–12.6 GHz, as shown in Fig. 5(a). However, the absorptivity decreases significantly in TM polarization, as shown in Fig. 5(b), due to the parallel direction of the magnetic field with the resistor surface.²⁰ Nevertheless, the absorptivity remains higher than 70% from 6.8 GHz to 11.8 GHz

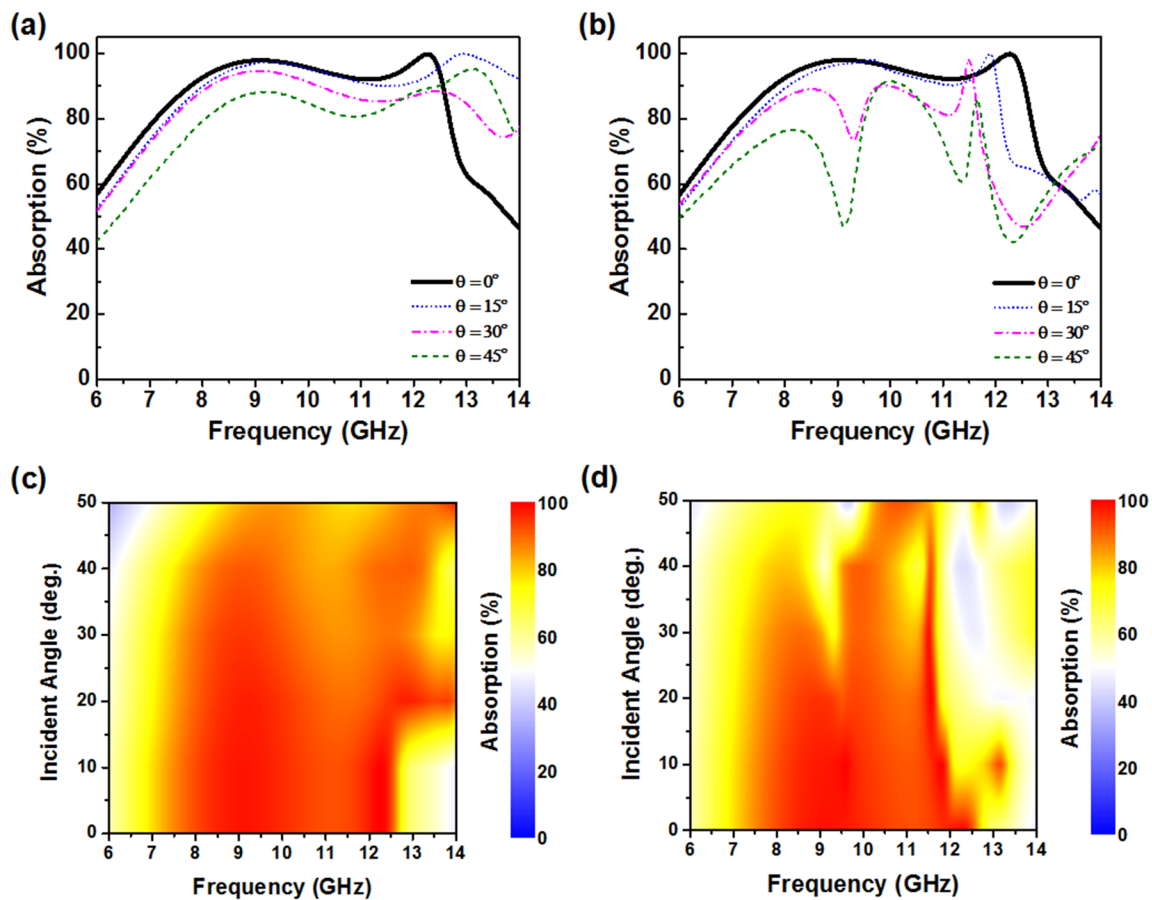


FIG. 5. Absorption spectra of the proposed MMA as a function of the incident angle of TE polarizations [(a) and (c)] and of TM polarizations [(b) and (d)].

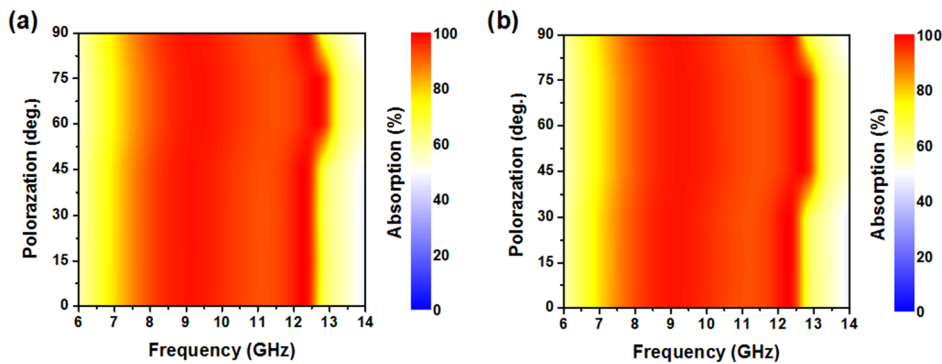


FIG. 6. Absorption spectra of the proposed MMA under normal incidence with (a) TE polarization and (b) TM polarizations.

at wide incident angles from 0° to 30° under both TE and TM polarizations. As for the polarization behavior of the MMA, as shown in Fig. 6, the absorption spectra are nearly unchanged at different polarization angles for both TE and TM polarizations under normal incidence. It indicates that the MMA has an insensitive polarization characteristic due to its symmetry structure.^{12,13}

To gain insights into the absorption mechanism, the distributions of electric and surface current of the proposed MMA are simulated under the TE polarization at the two resonant frequencies of 9.1 GHz and 12.2 GHz in the XOY plane under normal incidence. Figure 7(a) shows that at the resonant frequency of 9.1 GHz, the resonant absorption is mainly generated by the inner edge of the metallic SCR resonator, whereas Fig. 7(d) shows that at a higher resonant frequency, the resonant absorption is mainly caused by the gap of the SCR metallic resonator and the lumped resistors. It was also reported that the electric field distribution on the lumped resistors can be attributed to the broadband absorption property.^{20,21} At a lower frequency of 9.1 GHz, the top and the bottom surface currents are anti-parallel to each other, as seen

in Figs. 7(b) and 7(c), which confirm that the absorption mechanism is affected by magnetic resonance.^{47,48} Meanwhile, at a higher resonant frequency of 12.2 GHz, the surface currents are divided into three different regions, where the currents on adjacent regions are anti-parallel, as shown in Figs. 7(e) and 7(f), which form three current loops between the top and bottom metallic layers. Thus, a higher resonant frequency is due to the third-order magnetic resonance.^{49–51}

Finally, the absorption performance of the proposed MMA is compared with the other reported MMAs based on lumped resistors. Table I presents the MMA characteristics in terms of the number of layers, number of resistors, resonant frequency range, relative bandwidth, relative bandwidth per resistor, and thickness. It can be seen that the proposed MMA is a moderate structure, meaning it is not superior in all aspects; nevertheless, it is characterized by a simple structure and small thickness (0.109λ at the center absorption frequency) with a relatively high bandwidth per lumped resistor. Therefore, the proposed MMA can be very well suited for some practical applications that have a requirement matching its characteristics and performance.

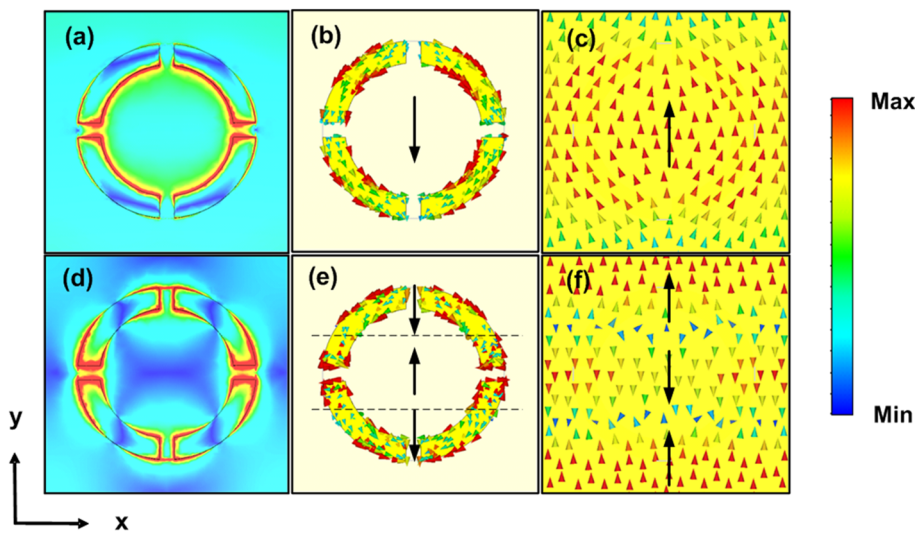


FIG. 7. [(a) and (d)] Distributions of electric field, [(b) and (e)] the top surface current, and [(c) and (f)] bottom surface current at various resonant frequencies of 9.1 GHz and 12.2 GHz.

TABLE I. Comparison of the performance of the proposed MMA with other reported MMAs. Boldface indicates the data determined in this work.

References	Number of layer	Number of resistor	Bandwidth (GHz)	Relative bandwidth (%)	Relative bandwidth per number of resistor	Thickness (mm)
20	1	8	8.2–13.5	48.8	6.1	3.0 (0.102 λ)
19	1	8	7.93–17.18	73.7	9.21	3.0 (0.126 λ)
39	1	8	8–18	76.9	9.6	10 (0.433 λ)
15	2	4	7.6–18.3	82.6	20.65	3.25 (0.14 λ)
40	3	6	6.79–14.96	75.1	12.52	5.6 (0.203 λ)
36	3	8	3–8	90.9	11.36	7.6 (0.139 λ)
41	3	12	5.2–18	110.3	9.19	4.6 (0.178 λ)
Proposed structure	1	4	7.8–12.6	47.0	11.75	3.2 (0.109λ)

CONCLUSION

A single layer broadband MMA based on a metal–dielectric–metal configuration for X-band applications was numerically designed. The MMA structure consisted of a periodic array of an SCR loaded with four lumped resistors to improve the bandwidth. A broadband absorption response of the MMA in the range of 7.8–12.6 GHz with absorptivity above 90% under normal incidence for all polarization angles was achieved. The MMA showed absorptivity above 70% in the frequency range of 6.8–11.8 GHz at wide incident angles from 0° to 30° for both TE and TM polarizations. The physical mechanism of the MMA design was investigated using electric and surface current distributions, significantly affected by the magnetic resonance.

ACKNOWLEDGMENTS

Data sharing is not applicable to this article as no new data were created or analyzed in this study.

REFERENCES

- B.-X. Wang, X. Zhai, G.-Z. Wang, W.-Q. Huang, and L.-L. Wang, “A novel dual-band terahertz metamaterial absorber for a sensor application,” *J. Appl. Phys.* **117**(1), 014504 (2015).
- Y. Zhang, J. Zhao, J. Cao, and B. Mao, “Microwave metamaterial absorber for non-destructive sensing applications of grain,” *Sensors* **18**(6), 1912 (2018).
- H. A. Atwater and A. Polman, “Plasmonics for improved photovoltaic devices,” *Nat. Mater.* **9**, 205–213 (2010).
- S. Mubeen, J. Lee, W. Lee, N. Singh, G. D. Stucky, and M. Moskovits, “On the plasmonic photovoltaic,” *ACS Nano* **8**(6), 6066–6073 (2014).
- T. Beeharry, R. Yahiaoui, K. Selemanni, and H. H. Ouslimani, “A dual layer broadband radar absorber to minimize electromagnetic interference in radomes,” *Sci. Rep.* **8**, 382 (2018).
- G. Sen, M. Kumar, S. N. Islam, and S. Das, “Broadband metamaterial absorber on a single-layer ultrathin substrate,” *Waves Random Complex Media* **29**(1), 153 (2019).
- N. I. Landy, S. Sajuyigbe, J. J. Mock, D. R. Smith, and W. J. Padilla, “Perfect metamaterial absorber,” *Phys. Rev. Lett.* **100**, 207402 (2008).
- Y. Liu, S. Gu, C. Luo, and X. Zhao, “Ultra-thin broadband metamaterial absorber,” *Appl. Phys. A* **108**(1), 19–24 (2012).

- W. Ma, Y. Wen, and X. Yu, “Broadband metamaterial absorber at mid-infrared using multiplexed cross resonators,” *Opt. Express* **21**(25), 30724–30730 (2013).
- D. T. Viet, N. T. Hien, P. V. Tuong, N. Q. Minh, P. T. Trang, L. N. Le, Y. P. Lee, and V. D. Lam, “Perfect absorber metamaterials: Peak, multi-peak and broadband absorption,” *Opt. Commun.* **322**(1), 209–213 (2014).
- Y. Cui, K. H. Fung, J. Xu, H. Ma, Y. Jin, S. He, and N. X. Fang, “Ultrabroadband light absorption by a sawtooth anisotropic metamaterial slab,” *Nano Lett.* **12**(3), 1443–1447 (2012).
- N. T. Q. Hoa, P. H. Lam, and P. D. Tung, “Wide-angle and polarization-independent broadband microwave metamaterial absorber,” *Microwave Opt. Technol. Lett.* **59**(5), 1157–1161 (2017).
- N. T. Q. Hoa, P. D. Tung, P. H. Lam, N. D. Dung, and N. H. Quang, “Numerical study of an ultrabroadband, wide-angle, polarization-insensitivity metamaterial absorber in the visible region,” *J. Electron. Mater.* **47**, 2634–2639 (2018).
- Y. Shang, Z. Shen, and S. Xiao, “On the design of single-layer circuit analog absorber using double-square-loop array,” *IEEE Trans. Antennas Propag.* **61**(12), 6022–6029 (2013).
- H. Chen, X. Yang, S. Wu, D. Zhang, H. Xiao, K. Huang, Z. Zhu, and J. Yuan, “Flexible and conformable broadband metamaterial absorber with wide-angle and polarization stability for radar application,” *Mater. Res. Express* **5**(1), 015804 (2018).
- L. L. Cong, X. Y. Cao, T. Song, J. Gao, and J. X. Lan, “Angular-and polarization-insensitive ultrathin double-layered metamaterial absorber for ultra-wideband application,” *Sci. Rep.* **8**, 9627 (2018).
- J. Chen, X. Huang, G. Zerihun, Z. Hu, S. Wang, G. Wang, X. Hu, and M. Liu, “Polarization-independent, thin, broadband metamaterial absorber using double-circle rings loaded with lumped resistances,” *J. Electron. Mater.* **44**, 4269–4274 (2015).
- M. Bağmancı, O. Akgöl, M. Özkürtük, M. Karaaslan, E. Ünal, and M. Bakır, “Polarization independent broadband metamaterial absorber for microwave applications,” *Int. J. RF Microwave Comput.-Aided Eng.* **29**, e21630 (2019).
- S. Li, J. Gao, X. Cao, W. Li, Z. Zhang, and D. Zhang, “Wideband, thin, and polarization-insensitive perfect absorber based the double octagonal rings metamaterials and lumped resistances,” *J. Appl. Phys.* **116**, 043710 (2014).
- T. T. Nguyen and S. Lim, “Design of metamaterial absorber using eight-resistive-arm cell for simultaneous broadband and wide-incidence-angle absorption,” *Sci. Rep.* **8**, 6633 (2018).
- T. T. Nguyen and S. Lim, “Angle-and polarization-insensitive broadband metamaterial absorber using resistive fan-shaped resonators,” *Appl. Phys. Lett.* **112**, 021605 (2018).
- D. K. Cheng, *Field and Wave Electromagnetics* (Addison-Wesley, 2011), p. 417.
- M. Aalizadeh, A. Khavasi, B. Butun, and E. Ozbay, “Large-area, cost-effective, ultra-broadband perfect absorber utilizing manganese in metal-insulator-metal structure,” *Sci. Rep.* **8**, 9162 (2018).

- ²⁴N. T. Q. Hoa, T. S. Tuan, L. T. Hieu, and B. L. Giang, "Facile design of an ultrathin broadband metamaterial absorber for C-band applications," *Sci. Rep.* **9**, 468 (2019).
- ²⁵C. Gong, M. Zhan, J. Yang, Z. Wang, H. Liu, Y. Zhao, and W. Liu, "Broadband terahertz metamaterial absorber based on sectional asymmetric structures," *Sci. Rep.* **6**, 32466 (2016).
- ²⁶See <http://www.cst.com/> for CST Computer Simulation Technology 3D EM Field Simulation.
- ²⁷F. Ding, Y. Cui, X. Ge, Y. Jin, and S. He, "Ultra-broadband microwave metamaterial absorber," *Appl. Phys. Lett.* **100**(10), 103506 (2012).
- ²⁸X. F. Zang, C. Shi, L. Chen, B. Cai, Y. M. Zhu, and S. L. Zhuang, "Ultra-broadband terahertz absorption by exciting the orthogonal diffraction in dumbbell-shaped gratings," *Sci. Rep.* **5**, 8901 (2015).
- ²⁹W. Xin, Z. Binzhen, W. Wanjuan, W. Junlin, and D. Junping, "Design, fabrication, and characterization of a flexible dual-band metamaterial absorber," *IEEE Photonics J.* **9**(4), 4600213 (2017).
- ³⁰M. C. Tran, D. H. Le, V. H. Pham, H. T. Do, D. T. Le, H. L. Dang, and V. D. Lam, "Controlled defect based ultra broadband full-sized metamaterial absorber," *Sci. Rep.* **8**, 9523 (2018).
- ³¹J. Ren and J. Y. Yin, "Cylindrical-water-resonator-based ultra-broadband microwave absorber," *Opt. Mater. Express* **8**, 2060–2071 (2018).
- ³²T. Beeharry, R. Yahiaoui, K. Selemani, and H. Ouslimani, "A co-polarization broadband radar absorber for RCS reduction," *Materials* **11**, 1668 (2018).
- ³³M. Bağmancı, M. Karaaslan, O. Altuntaş, F. Karadağ, E. Tetik, and M. Bakır, "Wideband metamaterial absorber based on CRRs with lumped elements for microwave energy harvesting," *J. Microwave Power Electromagn. Energy* **52**, 45–59 (2018).
- ³⁴T. S. Tuan, V. D. Lam, and N. T. Q. Hoa, "Simple design of a copolarization wideband metamaterial absorber for C-band applications," *J. Electron. Mater.* **48**, 5018–5027 (2019).
- ³⁵Y. J. Kim, J. S. Hwang, Y. J. Yoo, B. X. Khuyen, J. Y. Rhee, X. Chen, and Y. P. Lee, "Ultrathin microwave metamaterial absorber utilizing embedded resistors," *J. Phys. D: Appl. Phys.* **50**, 405110 (2017).
- ³⁶S. Zhong, W. Jiang, P. Xu, T. Liu, J. Huang, and Y. Ma, "A radar-infrared bistable structure based on metasurfaces," *Appl. Phys. Lett.* **110**, 063502 (2017).
- ³⁷D. Kundu, A. Mohan, and A. Chakrabarty, "Single-layer wideband microwave absorber using array of crossed dipoles," *IEEE Antennas Wireless Propag. Lett.* **15**, 1589–1592 (2016).
- ³⁸X. Huang, X. He, L. Guo, Y. Yi, B. Xiao, and H. Yang, "Analysis of ultra-broadband metamaterial absorber based on simplified multi-reflection interference theory," *J. Opt.* **17**, 055101 (2015).
- ³⁹J. Yang and Z. Shen, "A thin and broadband absorber using double-square loops," *IEEE Antennas Wireless Propag. Lett.* **6**, 388–391 (2007).
- ⁴⁰M. Yoo and S. Lim, "Polarization-independent and ultrawideband metamaterial absorber using a hexagonal artificial impedance surface and a resistor-capacitor layer," *IEEE Trans. Antennas Propag.* **62**(5), 2652–2658 (2014).
- ⁴¹S. Ghosh, S. Bhattacharyya, and K. V. Srivastava, "Design, characterisation and fabrication of a broadband polarisation-insensitive multi-layer circuit analogue absorber," *IET Microwaves, Antennas Propag.* **10**(8), 850–855 (2016).
- ⁴²F. Bilotti, A. Toscano, L. Vegni, K. Aydin, K. B. Alici, and E. Ozbay, "Equivalent circuit models for the design of metamaterials based on artificial magnetic inclusions," *IEEE Trans. Microwave Theory Tech.* **55**, 2865–2873 (2007).
- ⁴³Y. Z. Cheng, Y. Wang, Y. Nie, R. Z. Gong, X. Xiong, and X. Wang, "Design, fabrication and measurement of a broadband polarization-insensitive metamaterial absorber based on lumped elements," *J. Appl. Phys.* **111**(4), 044902 (2012).
- ⁴⁴S. Ghosh, S. Bhattacharyya, D. Chaurasiya, and K. V. Srivastava, "An ultrawideband ultrathin metamaterial absorber based on circular split rings," *IEEE Antennas Wireless Propag. Lett.* **14**, 1172–1175 (2015).
- ⁴⁵D. R. Smith, D. C. Vier, T. Koschny, and C. M. Soukoulis, "Electromagnetic parameter retrieval from inhomogeneous metamaterials," *Phys. Rev. E* **71**, 036617 (2005).
- ⁴⁶S. Bhattacharyya and K. V. Srivastava, "Triple band polarization-independent ultra-thin metamaterial absorber using electric field-driven LC resonator," *J. Appl. Phys.* **115**(6), 064508 (2014).
- ⁴⁷N. T. Q. Hoa, P. H. Lam, P. D. Tung, T. S. Tuan, and H. Nguyen, "Numerical study of a wide-angle and polarization-insensitive ultrabroadband metamaterial absorber in visible and near-infrared region," *IEEE Photonics J.* **11**(1), 4600208 (2019).
- ⁴⁸N. V. Dung, B. S. Tung, B. X. Khuyen, Y. J. Yoo, Y. J. Kim, J. Y. Rhee, V. D. Lam, and Y. P. Lee, "Simple metamaterial structure enabling triple-band perfect absorber," *J. Phys. D: Appl. Phys.* **48**(37), 375103 (2015).
- ⁴⁹N. V. Dung, P. V. Tuong, Y. J. Yoo, Y. J. Kim, B. S. Tung, V. D. Lam, J. Y. Rhee, K. W. Kim, Y. H. Kim, L. Y. Chen, and Y. P. Lee, "Perfect and broad absorption by the active control of electric resonance in metamaterial," *J. Opt.* **17**, 045105 (2015).
- ⁵⁰Y. J. Kim, Y. J. Yoo, K. W. Kim, J. Y. Rhee, Y. H. Kim, and Y. P. Lee, "Dual broadband metamaterial absorber," *Opt. Express* **23**, 3861 (2015).
- ⁵¹Y. Z. Cheng, Z. Z. Cheng, X. S. Mao, and R. Z. Gong, "Ultra-thin multi-band polarization-insensitive microwave metamaterial absorber based on multiple-order responses using a single resonator structure," *Materials* **10**, 1241 (2017).